NOVEL MUTATION ALTERS THE STRUCTURE AND FUNCTION OF THE ACTH RECEPTOR (MC2R) CAUSING A FAMILIAL GLUCOCORTICOID DEFICIENCY

Running Title:

Novel Mutation of the ACTH Receptor Gene (MC2R)

Rocío A. Artigas[1,*], Angel Gonzalez[5,*], Erick Riquelme[4], Cristian A. Carvajal[1,4], Andreína Cattani[2], Alejandro Martínez-Aguayo[2], Alexis M. Kalergis[3,4], Tomas Pérez-Acle[5,6] & Carlos E. Fardella[1,4]

Department of Endocrinology[1], Pediatrics[2] and Rheumatology[3], Facultad de Medicina.

Millennium Nucleus on Immunology and Immunotherapy[4], Departamento de Genética Molecular y Microbiología, Facultad de Ciencias Biológicas.

Centre for Bioinformatics (CBUC)[5], Facultad de Ciencias Biológicas,

Pontificia Universidad Católica de Chile

Fundación Ciencia para la Vida[6], Avda. Zañartu 1482, Ñuñoa, Santiago

Corresponding author:

Dr. Carlos E. Fardella, MD

Departamento de Endocrinología

Facultad de Medicina

Pontificia Universidad Católica de Chile

Lira 85, 5° piso

Santiago, Chile

Phone: + 056-2-354 30 95

Fax: + 056-2-638 56 75

E-mail: cfardella@med.puc.cl

(*) These authors have contributed equally to this work.

DISCLOSURE STATEMENT: The authors have nothing to disclose.

Word count: 3868

ABSTRACT.-
Familial Glucocorticoid Deficiency (FGD) is a rare autosomal recessive disorder. Here we report a 9 year-old boy with FGD. The family history showed non consanguineous healthy parents, 3 healthy siblings and one brother affected with FGD. The molecular studies demonstrated the presence of an adenine heterozygous insertion (InsA1347) in the ACTH receptor (MC2R) gene (G217fs) in both patients. This insertion is responsible of a frame shift mutation in one allele, and a premature stop codon codifying an aberrant receptor of 247 residues (27.2kDa). Beside to this finding, we found a novel heterozygous mutation Alanine 126 by Serine 126 (Ala126Ser). The heterozygous mutations Ala126Ser and G217fs were carried by the father and mother, respectively, in the absence of any measurable symptom of glucocorticoid deficiency. The Ala126Ser mutation was introduced in the MC2R cDNA by site-directed mutagenesis, cloned on an expression vector and transfected in CHO cells together with a cAMP-responsive luciferase reporter plasmid. The mutant MC2R-Ala126Ser showed a significant lower activity when it was stimulated with ACTH-(1-24) than did cells transfected with wild type MC2R. Molecular dynamics simulations conducted in comparative models of the wild type receptor and the Ala126Ser mutant showed that Ser126 side-chain fluctuates forming a non-canonical intrahelical hydrogen bond in the transmembrane helix (TMH) 3, near to the G-protein coupled receptor's highly conserved DRY motif. Ligand-binding site analyses performed over trajectory ensembles, revealed extensive structural rearrangements at the internal cavities of the Ala126Ser mutant that may affect the ligand recognition and signal transduction throughout G-protein.

Keywords: Compound Heterozygous Mutation/ Melanocortin Receptor/ Familial Glucocorticoid Deficiency, Molecular Dynamics, Comparative Modeling, GPCR.

INTRODUCTION.-

Familial glucocorticoid deficiency (FGD) is a rare autosomal recessive disorder in which secretion of cortisol and androgen is deficient and unresponsive to ACTH stimulation (1). Although symptoms of the disease are usually observed during the first year of life, they can also appear during infancy or later childhood with hyperpigmentation, muscle weakness, hypoglycemia, and seizures caused by low cortisol and elevated ACTH levels (2). It has been shown that inactivating mutations in the adrenal receptor for ACTH (melanocortin 2 receptor, MC2R) are found in about 40% of FGD kindreds (FGD type-1, OMIM #202200). Most mutations are missense and there is no specific hot spot for mutation. The small numbers of nonsense mutations, stop codons and frameshift mutations, occur as compound heterozygotes with a missense mutation in all but a few cases (3). In the remaining 60% of cases no mutations are identifiable in the MC2R gene (FGD type-2). Recent studies (4) have identified the gene encoding for a small single transmembrane domain protein known as melanocortin 2 receptor accessory protein (MRAP, OMIM *609196) as another underlying FGD type 2. This protein functions as an accessory protein for MC2R contributing in part to promote its expression at the cell´s surface. Mutations in MRAP account for the 20% of all FGD cases, implying that at least half of all FGD cases result from other genes yet to be identified (3).

The MC2R is the smaller member of the class A rhodopsin-like G protein-coupled receptors (GPCRs) family within which it joined the melanocortin 1, 3, 4 and 5 to form the melanocortin receptor (MCR) subgroup (5). In contrast to the other four MCRs, MC2R is only activated by ACTH, whereas the other MCRs can be activated by both ACTH and MSH (6). It is known that the binding of ACTH to MC2R activates the heterotrimeric G protein complex that induces adenylate cyclase to form cAMP, which stimulates steroidogenesis acutely through the action of the steroidogenic acute regulatory protein and chronically through transcriptionally induced accumulation of mRNAs for steroidogenic enzymes (7).

The human MC2R gene is in chromosome 18 and consists of 2 exons spaning about 1.1 kb. The only coding region is within the second exon which gives rise to a protein of 297 amino acids (3). The predicted protein for the MC2R had a molecular weight in its unmodified form of 33 kd. Available evidence supports the notion that all GPCRs share a common fold composed of seven TMHs of ~25 to 35 residues long (TMHs 1 to 7), that span the cellular membrane connected by three extracellular (EC 1 to 3) and three cytoplasmatic loops (IC 1 to 3) (8). The N-terminal region, which varies in length and function, is located on the extracellular side of the membrane, while the C-terminal region is on the intracellular side (9). In spite of the overall low sequence identity exhibited by multiple alignments of the Class A GPCRs sequences, the existence of highly conserved residues in their seven transmembrane spanning domains has allowed the development of comparative models based on the crystallographic X-ray data of the bovine rhodopsin as a structural template (10). This approach has been broadly used to gain insights on the biophysical properties of a variety of Class A family members and to provide support to site-directed mutagenesis experiments, being also the main source for structural hypotheses tending to characterize the transition between the ensemble of active and the inactive states of these receptors (11, 12). The recent release of two crystallographic structures of the human β2-Adrenergic receptor (13, 14), at different resolutions, increases the number of templates available for GPCRs comparative modeling. As expected these new structures have a similar arrangement of transmembrane helices as compared to the homologous structure of rhodopsin.

Here, we report a novel heterozygous mutation in the MC2R gene that shows reduced activity in comparison to wild type and seems to be responsible of the FGD phenotype. Molecular dynamics simulations performed in explicit membrane conditions, using comparative models of the wild type MC2R and the Ala126Ser mutant, permitted us to compose a structural hypothesis that could be used to explain this reduced activity.

PATIENTS AND METHODS.-

Clinical case and biochemical profile.

We present a male, who was born from non-consanguineous Chilean parents after an uneventful delivery. He was a term newborn, with

a birth weight of 3,220 g. During his first month of life he had generalized hyperpigmentation. His genitals showed a normal development for his age, without pubarche. No sign of achalasia or alacrimia were noted. At the age of 2 years he had hypoglycemia and pleuropneumoniae associated with shock. During this stress, the endocrinological analysis revealed extremely low basal cortisol <1.1 mcg/dL (< 27.59 nmol/L) and post 250 mcg ev ACTH 1.1 mcg/dL (30.35 nmol/L); with plasma renin activity 2.8 ng/mL*h (NV 1-2.5 ng/mL*h), ACTH 1047 pg/mL (236.28 pmol/L), 17 OH Progesterone <0.1 ng/dL and Testosterone < 10 ng/dL. Other causes of primary adrenal insufficiency were studied (15, 16), the adrenal antibody, IFA <1:4 (not detectable), normal concentrations of very long chain fatty acids (VLCFA) and normal brain magnetic resonance imaging. With the diagnosis of primary adrenal insufficiency, hydrocortisone replacement therapy was introduced (100 mg/m^2 during stress and then 10-12 mg/m^2*d). At the age of 2 years his height was 99 cm (99.9th percentile). The father's height was 190 cm (96.8th percentile), and mother's height: was 172 cm (91.0th percentile); and he had an accelerated bone age (BA) with a BA/CA=2 Moreover, his height velocity was 15 cm/year during the year before the diagnosis. The TSH was 5.57 mUI/mL (Normal range (NR); 0.49-6.1 mUI/mL) and normal free-T4 1.43 ng/dL (NR, 0.8-2,1 ng/dL). The level of IGF-1 was 158 ng/mL (NR, 17-248) and IGFBP-3 was 3.6 µg/ml (NR, 0.9- 4.1). The parents had ACTH, basal and post ACTH cortisol and PRA within the normal ranges, and were not affected with FGD. The youngest brother (6 months-old) was studied because of a generalized hyperpigmentation. He presented a low basal cortisol as 0.4 mcg/dL (< 27.59 nmol/L) with elevated ACTH plasma levels (1,250 pg/ml) associated with normal PRA (11.3 ng/ml/hr).

Analysis of genomic DNA

Genomic DNA was isolated from peripheral blood mononuclear cells obtained from the index case, his parents and siblings. DNA purification protocol was carried out using DNAzol reagent (Invitrogen Corp., San Diego, CA). The entire coding region of MC2R gene was amplified by conventional PCR using previously reported primers, MC2R-S and MC2R-AS primers (17) and procedures (18) (see SI. Materials and methods). PCR fragments were purified by Qiaquick gel extraction purification kit (Qiagen, USA) and directly sequenced in the ABI Prism 377 DNA genetic analyzer (Applied Biosystem, USA). The MC2R gene sequence was compared using BLASTn (19) with the nucleotide database available in GenBank (20). As a result, the complementary region that span from positions 13.894.624 to 13.875.517 nt of the chromosome locus 18p11.2 (GenBank accession: NM_000529) was obtained. This sequence was globally aligned to our MC2R gene sequence using ClustalW program (21), looking for genetic alterations.

Site directed mutagenesis and transient transfection

pcDNA3.1-MC2R plasmid, generously donated by Professor Walter L. Miller (University of California San Francisco, USA) was used to perform the *expression studies* and to generate the mutant MC2R cDNA (Ala126Ser) vector (7) by means of Site-directed mutagenesis system (Stratagene, USA) and oligonucleotides designed following the manufacturer´s instructions. The parental methylated wild type cDNA was digested with 10U DpnI at 37°C for 90 min, and the remaining unmethylated mutagenized cDNA plasmid was used to transform E. coli DH5 cells. The resulting mutagenized plasmids were sequenced in an automatic analyzer to confirm the presence of the required mutation. CHO cells, which do not express MC2R gene by themselves, were cultured in 24-well plates 48 h before transfection at approximately 80% confluence. Prior to transfection, the cells were maintained in a medium supplemented without antibiotic. Cells were incubated overnight with DNA-Lipofectamine™ 2000 complexes containing vectors expressing wild type or mutant MC2R cDNA or an equal mass of empty pcDNA3 plus a cAMP-responsive luciferase reporter plasmid (pCREluc) that contained 16 cAMP response element units. At the end of the incubation, the DNA-Lipofectamine 2000 complexes were removed and the cells were incubated in a fresh medium for 36 h to allow gene expression before stimulation with synthetic ACTH-(1-24) (Sigma, USA). Forty-eight hrs after the transfection and before the incubation with ACTH some wells were removed to evaluate receptor expression wild

type or mutant MC2R on the cells surface transfected. This was assessed through flow cytometry by staining it with Rabbit Anti-Mouse MC2R Polyclonal Antibody, unconjugated (H-70) (Santa Cruz Bitechnology, INC) following by Goat Anti-Rabbit IgG-PE (Pierce). The remaining wells were then incubated with 10^{-7} M ACTH-(1-24) for 18h at 37º C in 5% CO_2. As positive control we used 1 mM 8-bromo-cAMP because pCREluc is activated by cAMP. Cells were lysed and assayed for luciferase activity using the Luciferase assay kit (Stratagene). Cotransfection of ß-galactosidase reporter vector was used as the transfection efficiency control and the results were expressed as activity Luc/activity ß-gal.

q*PCR of MC2R*

Total RNA was extracted with TRIZOL LS reagent (Invitrogen, USA). RNA (2 µg) was reversely transcribed using the StrataScipt RT (Stratagen, USA) and random primers. For real-time PCR (qPCR), 2 ul of total cDNA were amplified with QuantiSyg (Quantimix Easy SYG kit, BioTools B&M Labs, Spain) and gene specific primers (Q-MC2R-S and Q-MC2R-AS) (see SI Materials and Methods). Reaction conditions were 3 min at 95 C followed by 35 cycles of 15 sec at 95 and 30 sec at 60 in a Rotor-Gene 6000 (Corbett, Australia). Real-time PCR (qPCR) data was obtained during the extension phase and threshold cycle values were obtained at the log phase of each gene amplification. PCR product quantification was performed by the relative quantification method (22) and standardized against human GAPDH or 18S RNA. Efficiency for each primer pair was assessed by using serial dilutions of RT product.

Sequence alignment and MC2R comparative modeling

In order to produce a MC2R molecular model, the highest-resolution 2.2 Å crystal structure of bovine rhodopsin (PDBid: 1U19) was used as a template for comparative modeling (23). MC2R and rhodopsin sequences were aligned using the available information of highly conserved residues shared within the GPCRs (9) (see SI Fig. I). This alignment was used as an input to MODELLER v8 (24) to develop a total of 100 comparative models that were ranked with the highest level of quality (25, 26). The best evaluated structure was selected for further refinement. A Ala126Ser mutant model was produced using the BuildMutant module available within MODELLER v8, being subsequently energy optimized using the loop optimization procedure available in this program.

Molecular dynamic simulations in explicit membrane environment.

The MC2R wild type and the Ala126Ser mutant models (see SI Fig. II) were independently embedded in a pre-equilibrated lipid bilayer consisting of 288 molecules of 1,2-Dipalmitoylphosphatidylcholine (DPPC) (27). Insertion of the alpha helical bundle into the lipid core was adjusted to obtain both the TMH4 and the cytosolic half of THM6 perpendicular to the membrane plane (28, 29). Protein-overlapping lipids were subsequently removed. Final systems dimension resulted in a periodic box of 98 x 98 x 112 (Å) with a total of 98.418 atoms (see Fig. 1). Simulations were carried out using the NAMD v 2.6 MD package (30) using the TIP3 water model and the CHARMM22 all-hydrogen parameter file for proteins (31) and the CHARMM27 all-hydrogen force field for lipid parameter (32). Long-range electrostatic interactions were calculated using the particle mesh Ewald method (PME) to get a uniform charge density average area during simulation (33). Lennard-Jones and short-range neighbor list for Coulombic interactions were set at 12 Å. Simulations were performed under the NPT ensemble at 1 Atm using a Langevin piston. To compensate the net charge of the protein-membrane systems, Na+ and Cl- ions were added to reach an ionic concentration of 0.1mol/l. Temperature was controlled by a 310K temperature bath using a Langevin damping algorithm. Energy minimization to reduce close contacts was achieved through the steepest-descent algorithm. The energy minimized systems were then pre-equilibrated (0.3ns), being subsequently subjected to a 5 ns MD simulation at 310K with 1fs timestep. Trajectory frames were saved each 10 ps.

Statistical Analysis

Statistical analyses were performed using a one way ANOVA test, followed by Bonferroni`s Multiple Comparison test. Values were considered

statistically significant for $p \leq 0,05$.

RESULTS.-

Clinical studies

The diagnosis of FGD was suspected on the basis of a low or undetectable plasma cortisol, a markedly elevated plasma ACTH and normal electrolytes with a normal renin and aldosterone (34). The other laboratory studies supported the exclusion of adrenoleukodystrophy, congenital adrenal hyperplasia and autoimmune Addison´s disease. The triple A syndrome was excluded by the absence of achalasia, alacrimia and unexplained neurological defects (35). As the index case is a boy presenting prepubertal genitalia, normal PRA and tall stature, we focused our attention in the MC2R receptor gene.

Molecular studies

Sequencing analysis of the MC2R gene of the affected child revealed two different heterozygous mutations in the coding sequence: a heterozygous insertion of an adenine at position 1347 InsA1347Het (G217fs) and a alanine to serine substitution at position 126. The insertion would produce a frame shift mutation in one allele, and a premature stop codon codifying an aberrant receptor of 247aa (27.2kDa), instead of the 297aa normal receptor (32.7kDa). This mutation was also present in the index case's affected brother and also in their mother (Fig. 2a). The second mutation corresponds to a guanine to thymidine change. This is a novel mutation that results in the amino acid change; Alanine126 to Serine (Ala126Ser), Het(GCG/TCG). This substitution was also present in the affected brother and in their father's DNA (Fig. 2b). Either, father and mother carry one of the heterozygous mutations, Ala126Ser and InsA1347Het (G217fs) respectively, without symptoms of glucocorticoid deficiency. We found that the index case in our study and his affected younger brother, who manifest the glucocorticoid deficiency, present both mutations together in their DNA.

Expression studies

To determine the functional consequences of the Ala126Ser substitution we constructed expression vectors to produce the normal and mutant MC2R proteins in suitable mammalian cells. These vectors were used to transfect CHO cells which do not express MC2R. qPCR analysis indicated similar expression of MC2R RNA from both constructs (data not shown). We then evaluated the surface expression of both wild type and Ala126Ser MC2R through flow cytometry. These results show that in both conditions there is an equivalent amount of MC2R in the cell surface (Fig.3 a). To test the activity of the Ala126Ser mutation, CHO cells were transfected with MC2R wild type, MC2R-Ala126Ser and cotransfected with pCREluc and incubated with synthetic ACTH-(1-24). CHO cells cotransfected with pCREluc and the vector for MC2R wild type had a robust response to 10-7M ACTH-(1–24), but cells cotransfected with pCREluc and mutated MC2R had a lower activity than the former, when stimulated with ACTH-(1-24) (Fig.3 b). The empty pcDNA3.1 vector had no response. Furthermore, the activity of luciferase was measured in unstimulated cells or after stimulation with 1 mM 8-bromo-cAMP that served as the ACTH independent positive control. We also performed a full dose response curve and the differences observed previously were maintained throughout the different doses evaluated (SI. Fig. III).

Molecular Modeling and Dynamics Simulation

The initial global alignment of the MC2R sequence with the rhodopsin template was tailored using highly conserved residues present in all TMHs that are shared by the Class A GPCR family (see SI Fig. I). To accomplish with experimentally obtained suggestions, an s-s disulphide bridge was included between Cys245 and C251 in the comparative modeling step (36). With the aim to find a putative structural based explanation to the reduced activity showed by the Ala126Ser substitution, a mutant model was derived from the MC2R wild type structure (SI. Fig. II). The mutated residue (Ser126) was located just above the highly conserved DRY motif in the TMH 3 (37), and placed in the i-2 position from the most conserved residue R3.50 (in accordance with Ballesteros notation (38)). Due to the alpha helix periodicity, its position resulted on the opposite of the internal receptor vestibule with its polar lateral chain oriented towards the membrane lipid environment. This interesting issue resulted in contrast to the majority of GPCRs that exhibit hydrophobic residues in this region (9). To gain

insights into the dynamic effects of this single substitution, both the MC2R wild type and MC2R-Ala126Ser mutant models were independently embedded in a DPPC pre-equilibrated lipid bilayer and subjected to MD simulations. Figure 4a shows the Cα RMSD computed along the 5 ns trajectory for the two systems. As seen, the main structural variation along the MD simulations corresponds to loop regions, while the TMHs remain mostly stable under 3Å of spatial fluctuation. This result supports the notion that the MC2R wild type and mutant models resulted in stable structures, suitable to perform further biophysical analyses.

The behavior of the Ser126 polar lateral chain in a hydrophobic environment was studied by computing the χ1 angle fluctuation along the MD simulation, as can be seen in Figure 4b. This analysis revealed a transient shift of χ1 angle that is correlated with the formation of an intrahelical hydrogen bond between the Ser126(Oγ) atom and the i-4 carbonyl oxygen of Ser122, as can be seen in Figure 4c. With the aim to reveal the effects of the χ1 angle transient shift, we proceed to compute the volume of the receptor cavities using the average structures of the MC2R wild type and Ala126Ser mutant, extracted from the MD simulation trajectory (Fig. 5a and b). For comparative purposes, we repeated this calculation using two discrete structures of the wild type and mutant models, obtained at 3 ns of simulation, where the Ser126(Oγ) atom resulted in the trans orientation, as can be deduced in Figure 4b. As depicted, a comparative analysis between average ensembles of the MC2R wild type and the Ala126Ser models resulted in significant volumetric variations to the extent that the three cavities available in the wild type model were transformed into 5 cavities; two at the extracellular side and three at the intracellular side on the Ala126Ser receptor (see Fig. 5a and b). It is interesting to note that the wild type model obtained at 3ns of simulation time (Fig. 5c), mostly conserve the binding cavities configuration available in the average wild type structure (Fig. 5a) showing minor volumetric variations, as seen in Table 1. In contrast, the Ala126Ser mutant model obtained at the same simulation time (Fig. 5d) showed significant variations in the number and volume of the available binding cavities, in comparison with the average ensemble of the Ala126Ser mutant (Fig. 5b). Table 1 shows the volume per cavity available in the wild type and the mutant average models, and also for the selected representatives of both models at 3ns of simulation time. As can be noted, the average ensemble of the Ala126Ser mutant presents a compartmentalized and diminished binding site at both sides of the receptor that is not compensated even by summing the available volume cavities.

DISCUSSION.-

In this study we described a novel MC2R gene mutation and predicted the resulting MC2R 3-D structure, in a compound heterozygous patient with FGD phenotype due to InsA1347 (maternal) and Ala126Ser (paternal).

Either, father and mother carry one of the heterozygous mutations, Ala126Ser and insA1347 (G217fs) respectively, without symptoms of glucocorticoid deficiency confirming an autosomal recessive mode of inheritance and indicating that mutations of the ACTH receptor is the cause of the disorder within this family. Most of the clinical features in FGD can be explained by MC2R gene mutations (39). A MC2R KO mice model has been recently published. The disruption of MC2R in these pups leads to neonathal lethality in 75% of the cases, and those surviving to adulthood resemble many features observed in FGD patients such as undetectable levels of corticosterone (cortisol) despite high levels of ACTH, unresponsiveness to ACTH, and hypoglycemia (40).

However, the mechanism underlying the increased growth reported in several patients with MC2R mutations is unclear and is not associated with abnormalities in the GH/IGF-I axis. Tall stature is specifically associated with MC2R mutations and is not found in other forms of Addison´s disease. However, tall stature is also found in patients with MC4R mutations typically presenting with severe obesity (body mass index >40 kg/m2) and normal adrenal function (41).

The first mutation was already described, corresponding to InsA 1347 (G217fs), produces a frame shift loss, generating a premature stop codon and an aberrant receptor (42). InsA1347mutation lies in the third cytoplasmic loop near the sixth transmembrane helix (6). The premature termination introduced by this mutation would eliminate the entire TMH 7 of the receptor

molecule, including the highly conserved NPxxY-motif that plays an essential role in the GPCRs structure and function (43). Thus, a complete lost of activity for this mutation is expected. The second mutation is a novel mutation, corresponding to a guanine to thymidine change, converts Ala126 to Ser causing the substitution of an apolar (alanine) for a polar (serine) amino acid. This mutation is located at the cytoplasmatic end of TMH3.

In our study the functional consequences of the novel mutation Ala126Ser were evaluated in an assay activity of MC2R in vitro suggesting that the novel mutation Ala126Ser is impairing the functionality of the receptor approximately 40%. This loss of functionality is not due to lower surface expression as can be seen in Figure 3a.

To date more than thirty MC2R mutations have been described: missense, benign polymorphisms, nonsense or frame shift mutations, many of which are included in the Human Gene Mutation Database (www.hgmd.cf.ac.uk) (44). The functional consequences of a number of these mutations have been studied *in vitro* and include a loss of ligand binding or affinity, truncated receptors (resulting from frame shift mutation), disruption of TMHs, and a loss of signal transduction (6).

Based on our modeling and simulation results we propose that the lateral side chain of the Ser126 residue become exposed to the lipid environment in the MC2R mutant. As seen in Figure 4b, a transient shift of the Ser126 χ1 angle can be depicted along the MD simulation. This shift is correlated with the formation of an intra-helical hydrogen bond between the Ser126 hydroxyl group and the carbonyl oxygen of Ser122 (Figure 4c). Similar Ser χ1 (*trans – gauche*) shift variations have been described before, where serine is able to act as a hinge residue that affects the conformation of an α helix via an intrahelical hydrogen bond between the Oγ atom and the i-3 or i-4 carbonyl oxygen of the helix backbone (45). This shift is particularly important for other GPCRs where serine substitutions could induce perturbations in the TMHs (46) and lead to constitutive activity for some receptors (47). In this case, the mutation proximal to the conserved TMH3 DRY motif, become particularly relevant if we consider the multiple evidence that supports the important role of TMHs 3 and 6, in the activation of various class A GPCRs (48-51). Thus, it is expected that perturbations in the structure of TMHs, close to a functionally conserved region as DRY, conforms a scenario where some conformational changes could compromise the activation process (52). In searching for these changes, a binding site analysis was performed using MD representative structures of both, wild type and Ala126Ser mutant MC2R models, results that can be reviewed in Figure 5a to d and also in Table 1. As depicted, there are important differences in the volume, number and disposition of the internal cavities between the wild type and mutant average models (Fig. 5a and b). These differences become less significant when comparing the wild type and the mutant model at 3ns where the Ser126 χ1 angle exhibits a *trans* orientation (Fig. 5c and d). This data as a whole, suggests that the set of observed changes could be related to the Ser126 χ1 angle (*trans – gauche*) shift produced along the fluctuation dynamics of the mutant MC2R. Moreover, due to the transient nature of the χ1 angle shift (Fig. 4b), it is expected that the MC2R Ala126Ser mutant could fluctuate within a set of intermediate states where some functionality is retained.

In summary, we report a case of FGD associated to a novel Ala126Ser mutation that impairs the functionality of the ACTH receptor. The MC2R structure modeling suggests that the Ala126Ser mutation induces a perturbation in TMH 3 that could be related to the observed changes in the number and disposition of the receptor internal cavities. These observations as a whole, propose a suitable molecular explanation for the reduced activity exhibited by the MC2R Ala126Ser mutant.

ACKNOWLEDGMENTS

This work was supported by Chilean grant FONDECYT 1040834-1070876 (RA, CC, CF), Millennium Nucleus on Immunology and Immunotherapy (P04/030-F) (CC, CF, ER, AK), and Chilean Foundation for Cellular Biology and the Fundación Ciencia para la Vida, Chile (TPA, AG). AG and ER are CONICYT doctoral fellowship.

References:

1. **Fujieda K, Tajima T** 2005 Molecular basis of adrenal insufficiency. Pediatric research 57:62R-69R
2. **Tsigos C** 2002 in Hormone Resistance and Hypersensitivity States. EdGeorge P Chrousos (Lippincott Williams and Wilkins):447-453.
3. **Clark AJL, Metherell LA, Cheetham ME, Huebner A** 2005 Inherited ACTH insensitivity illuminates the mechanisms of ACTH action. Trends in Endocrinology & Metabolism 16:451-457
4. **Metherell LA, Chapple JP, Cooray S, David A, Becker C, Ruschendorf F, Naville D, Begeot M, Khoo B, Nurnberg P, Huebner A, Cheetham ME, Clark AJ** 2005 Mutations in MRAP, encoding a new interacting partner of the ACTH receptor, cause familial glucocorticoid deficiency type 2. Nature genetics 37:166-170
5. **Foord SM, Bonner TI, Neubig RR, Rosser EM, Pin JP, Davenport AP, Spedding M, Harmar AJ** 2005 International Union of Pharmacology. XLVI. G protein-coupled receptor list. Pharmacol Rev 57:279-288
6. **Metherell LA, Chan LF, Clark AJ** 2006 The genetics of ACTH resistance syndromes. Best Pract Res Clin Endocrinol Metab 20:547-560
7. **Fluck CE, Martens JWM, Conte FA, Miller WL** 2002 Clinical, Genetic, and Functional Characterization of Adrenocorticotropin Receptor Mutations Using a Novel Receptor Assay. J Clin Endocrinol Metab 87:4318-4323
8. **Baldwin JM, Schertler GF, Unger VM** 1997 An alpha-carbon template for the transmembrane helices in the rhodopsin family of G-protein-coupled receptors. J Mol Biol 272:144-164
9. **Horn F, Bettler E, Oliveira L, Campagne F, Cohen FE, Vriend G** 2003 GPCRDB information system for G protein-coupled receptors. Nucleic Acids Res 31:294-297
10. **Filipek S, Teller DC, Palczewski K, Stenkamp R** 2003 The crystallographic model of rhodopsin and its use in studies of other G protein-coupled receptors. Annu Rev Biophys Biomol Struct 32:375-397
11. **Fanelli F, De Benedetti PG** 2005 Computational modeling approaches to structure-function analysis of G protein-coupled receptors. Chem Rev 105:3297-3351
12. **Reggio PH** 2006 Computational methods in drug design: modeling G protein-coupled receptor monomers, dimers, and oligomers. Aaps J 8:E322-336
13. **Cherezov V, Rosenbaum DM, Hanson MA, Rasmussen SG, Thian FS, Kobilka TS, Choi HJ, Kuhn P, Weis WI, Kobilka BK, Stevens RC** 2007 High-Resolution Crystal Structure of an Engineered Human {beta}2-Adrenergic G Protein Coupled Receptor. Science 318:1258-1265
14. **Rasmussen SG, Choi HJ, Rosenbaum DM, Kobilka TS, Thian FS, Edwards PC, Burghammer M, Ratnala VR, Sanishvili R, Fischetti RF, Schertler GF, Weis WI, Kobilka BK** 2007 Crystal structure of the human beta(2) adrenergic G-protein-coupled receptor. Nature 450:383-387
15. **Arlt W, Allolio B** 2003 Adrenal insufficiency. The Lancet 361:1881-1893
16. **Perry R, Kecha O, Paquette J, Huot C, Van Vliet G, Deal C** 2005 Primary adrenal insufficiency in children: twenty years experience at the Sainte-Justine Hospital, Montreal. J Clin Endocrinol Metab 90:3243-3250
17. **Sandrini F, Farmakidis C, Kirschner LS, Wu SM, Tullio-Pelet A, Lyonnet S, Metzger DL, Bourdony CJ, Tiosano D, Chan WY, Stratakis CA** 2001 Spectrum of mutations of

the AAAS gene in Allgrove syndrome: lack of mutations in six kindreds with isolated resistance to corticotropin. J Clin Endocrinol Metab 86:5433-5437

18. **Wu SM, Stratakis CA, Chan CH, Hallermeier KM, Bourdony CJ, Rennert OM, Chan WY** 1998 Genetic heterogeneity of adrenocorticotropin (ACTH) resistance syndromes: identification of a novel mutation of the ACTH receptor gene in hereditary glucocorticoid deficiency. Mol Genet Metab 64:256-265
19. **Altschul SF, Madden TL, Schaffer AA, Zhang J, Zhang Z, Miller W, Lipman DJ** 1997 Gapped BLAST and PSI-BLAST: a new generation of protein database search programs. Nucleic Acids Res 25:3389-3402
20. **Benson DA, Boguski MS, Lipman DJ, Ostell J, Ouellette BF, Rapp BA, Wheeler DL** 1999 GenBank. Nucleic Acids Res 27:12-17
21. **Thompson JD, Higgins DG, Gibson TJ** 1994 CLUSTAL W: improving the sensitivity of progressive multiple sequence alignment through sequence weighting, position-specific gap penalties and weight matrix choice. Nucleic Acids Res 22:4673-4680
22. **Pfaffl MW** 2001 A new mathematical model for relative quantification in real-time RT-PCR. Nucleic Acids Res 29:e45
23. **Okada T, Sugihara M, Bondar AN, Elstner M, Entel P, Buss V** 2004 The retinal conformation and its environment in rhodopsin in light of a new 2.2 A crystal structure. J Mol Biol 342:571-583
24. **Sali A, Blundell TL** 1993 Comparative protein modelling by satisfaction of spatial restraints. J Mol Biol 234:779-815
25. **Sippl MJ** 1993 Recognition of errors in three-dimensional structures of proteins. Proteins 17:355-362
26. **Eisenberg D, Luthy R, Bowie JU** 1997 VERIFY3D: assessment of protein models with three-dimensional profiles. Methods Enzymol 277:396-404
27. **Feller SE, Venable RM, Pastor RW** 1997a Computer Simulation of a DPPC Phospholipid Bilayer: Structural Changes as a Function of Molecular Surface Area. Langmuir 13:6555-6561
28. **Palczewski K, Kumasaka T, Hori T, Behnke CA, Motoshima H, Fox BA, Le Trong I, Teller DC, Okada T, Stenkamp RE, Yamamoto M, Miyano M** 2000 Crystal structure of rhodopsin: A G protein-coupled receptor. Science 289:739-745
29. **Li J, Edwards PC, Burghammer M, Villa C, Schertler GF** 2004 Structure of bovine rhodopsin in a trigonal crystal form. J Mol Biol 343:1409-1438
30. **Phillips JC, Braun R, Wang W, Gumbart J, Tajkhorshid E, Villa E, Chipot C, Skeel RD, Kale L, Schulten K** 2005 Scalable molecular dynamics with NAMD. J Comput Chem 26:1781-1802
31. **MacKerell J, A. D., Bashford D, Bellott MDJ, R.L., Evanseck JD, Field MJ, Fischer S, Gao J, Guo H, Ha S, Joseph-McCarthy D, Kuchnir L, Kuczera K, Lau FTK, Mattos C, Michnick S, Ngo T, Nguyen DT, Prodhom B, Reiher I, W.E., Roux B, Schlenkrich M, Smith JC, Stote R, Straub J, Watanabe M, Wiorkiewicz-Kuczera J, Yin DK, M.** 1998 All-atom empirical potential for molecular modeling and dynamics Studies of proteins. . Journal of Physical Chemistry B 102:3586-3616
32. **Feller S, MacKerell J, A.D.** 2000 An Improved Empirical Potential Energy Function for Molecular Simulations of Phospholipids. Journal of Physical Chemistry B 104:7510-7515
33. **Patra M, Karttunen M, Hyvonen MT, Falck E, Lindqvist P, Vattulainen I** 2003 Molecular dynamics simulations of lipid bilayers: major artifacts due to truncating electrostatic interactions. Biophys J 84:3636-3645

34. **Zennaro MC** 1998 Syndromes of glucocorticoid and mineralocorticoid resistance. Eur J Endocrinol 139:127-138
35. **Elias LL, Huebner A, Metherell LA, Canas A, Warne GL, Bitti ML, Cianfarani S, Clayton PE, Savage MO, Clark AJ** 2000 Tall stature in familial glucocorticoid deficiency. Clin Endocrinol (Oxf) 53:423-430
36. **Yang Y, Chen M, Kesterson RA, Jr., Harmon CM** 2007 Structural insights into the role of the ACTH receptor cysteine residues on receptor function. Am J Physiol Regul Integr Comp Physiol 293:R1120-1126
37. **Rovati GE, Capra V, Neubig RR** 2007 The highly conserved DRY motif of class A G protein-coupled receptors: beyond the ground state. Molecular pharmacology 71:959-964
38. **Ballesteros JA, Weinstein H** 1995 Integrated Methods for the Construction of Three-Dimensional Models and Computational Probing of Structure Function Relations in G Protein-Coupled Receptors. Methods in Neuroscience 25:366-428
39. **Weber A, Toppari J, Harvey RD, Klann RC, Shaw NJ, Ricker AT, Nanto-Salonen K, Bevan JS, Clark AJ** 1995 Adrenocorticotropin receptor gene mutations in familial glucocorticoid deficiency: relationships with clinical features in four families. J Clin Endocrinol Metab 80:65-71
40. **Chida D, Nakagawa S, Nagai S, Sagara H, Katsumata H, Imaki T, Suzuki H, Mitani F, Ogishima T, Shimizu C, Kotaki H, Kakuta S, Sudo K, Koike T, Kubo M, Iwakura Y** 2007 Melanocortin 2 receptor is required for adrenal gland development, steroidogenesis, and neonatal gluconeogenesis. Proc Natl Acad Sci U S A 104:18205-18210
41. **Lubrano-Berthelier C, Cavazos M, Dubern B, Shapiro A, Stunff CL, Zhang S, Picart F, Govaerts C, Froguel P, Bougneres P, Clement K, Vaisse C** 2003 Molecular genetics of human obesity-associated MC4R mutations. Annals of the New York Academy of Sciences 994:49-57
42. **Naville D, Barjhoux L, Jaillard C, Faury D, Despert F, Esteva B, Durand P, Saez J, Begeot M** 1996 Mutations of ACTH receptor gene and familial syndrome of glucocorticoid deficiency. Ann Endocrinol (Paris) 57:101-106
43. **Karnik SS, Gogonea C, Patil S, Saad Y, Takezako T** 2003 Activation of G-protein-coupled receptors: a common molecular mechanism. Trends in endocrinology and metabolism: TEM 14:431-437
44. **Stenson PD, Ball EV, Mort M, Phillips AD, Shiel JA, Thomas NS, Abeysinghe S, Krawczak M, Cooper DN** 2003 Human Gene Mutation Database (HGMD): 2003 update. Hum Mutat 21:577-581
45. **Ballesteros JA, Deupi X, Olivella M, Haaksma EE, Pardo L** 2000 Serine and threonine residues bend alpha-helices in the chi(1) = g(-) conformation. Biophys J 79:2754-2760
46. **Zhang R, Hurst DP, Barnett-Norris J, Reggio PH, Song ZH** 2005 Cysteine 2.59(89) in the second transmembrane domain of human CB2 receptor is accessible within the ligand binding crevice: evidence for possible CB2 deviation from a rhodopsin template. Molecular pharmacology 68:69-83
47. **Ambrosio C, Molinari P, Cotecchia S, Costa T** 2000 Catechol-binding serines of beta(2)-adrenergic receptors control the equilibrium between active and inactive receptor states. Molecular pharmacology 57:198-210
48. **Ballesteros JA, Jensen AD, Liapakis G, Rasmussen SG, Shi L, Gether U, Javitch JA** 2001 Activation of the beta 2-adrenergic receptor involves disruption of an ionic lock between the cytoplasmic ends of transmembrane segments 3 and 6. J Biol Chem 276:29171-29177

49. **Ghanouni P, Steenhuis JJ, Farrens DL, Kobilka BK** 2001 Agonist-induced conformational changes in the G-protein-coupling domain of the beta 2 adrenergic receptor. Proc Natl Acad Sci U S A 98:5997-6002

50. **Greasley PJ, Fanelli F, Rossier O, Abuin L, Cotecchia S** 2002 Mutagenesis and modelling of the alpha(1b)-adrenergic receptor highlight the role of the helix 3/helix 6 interface in receptor activation. Molecular pharmacology 61:1025-1032

51. **Ward SD, Hamdan FF, Bloodworth LM, Siddiqui NA, Li JH, Wess J** 2006 Use of an in situ disulfide cross-linking strategy to study the dynamic properties of the cytoplasmic end of transmembrane domain VI of the M3 muscarinic acetylcholine receptor. Biochemistry 45:676-685

52. **D'Antona AM, Ahn KH, Wang L, Mierke DF, Lucas-Lenard J, Kendall DA** 2006 A cannabinoid receptor 1 mutation proximal to the DRY motif results in constitutive activity and reveals intramolecular interactions involved in receptor activation. Brain Res 1108:1-11

Figure Legends

Fig. 1. DPPC-MC2R molecular system [98 x 98 x 112] (Å) with a total of 98.418 atoms. The thickness of the water layer was 30Å on both sides of the lipid bilayer. Lateral (**a**) and extracellular (**b**) views of the lipid receptor system after 5 ns MD simulation. Wild type MC2R receptor appears in golden ribbons and lipids in grey licorice. The blue surface points represent water molecules in (**a**) and were excluded in (**b**). Ions are displayed in red.

Fig. 2. Panel a, sequence analysis and identification of the MC2R insertion (InsA1347). DNA sequences of controls, heterozygous not affected (mother) and compound heterozygous affected patients (the index case and his youngest brother) are shown. **Panel b**, sequence analysis and identification of the MC2R mutation Ala126Ser. DNA sequences of controls, heterozygous not affected (father) and compound heterozygous affected patients (the index case and his youngest brother) are shown.

Fig. 3. **Panel a**, Analysis receptor expression. The surface expression of both wild type and Ala126Ser MC2R was assessed through flow cytometry. **Panel b**, Luciferase Activity Assays. CHO cells were transfected with the vector pcDNA3.1 expressing the wild type MC2R cDNA and mutant MC2R(Ala126Ser) cDNA and cotransfected with the reporter plasmid pCREluc cDNA or with an equal mass of empty pcDNA3.1. Luciferase activity was measured in unstimulated cells or after stimulation with 1mM 8-bromo-cAMP or 10-7 M ACTH-(1–24) overnight. Cells transfected with the empty pcDNA3.1 vector served as control. Values are expressed as the mean SEM of three independent transfection experiments, each performed in triplicate. Statistical differences were assessed through a one way ANOVA followed by Bonferroni´s multiple comparison test. Legend: *, $p \leq 0,05$; **, $p \leq 0,01$; ***, $p \leq 0,001$; n.s., non significant

Fig. 4. MD Simulations of MC2R models in explicit lipid environment. **Panel a**, Root mean square deviation (RMSD) of the MC2R wild type and (Ala126Ser) protein backbones during simulation. The RMSD values for TMHs and loops regions are displayed separately. **Panel b**, conformational preference calculated for the Ser126 $\chi 1$ torsion angle along the MD simulation. **Panel c**, distance between the Ser126 (Oγ) atom and the carbonyl oxygen (O) of Ser122 along the 5ns MD trajectory. In the figure is also shown a longitudinal view of the TMH3 C-terminal region at 1, 3 and 5ns of simulation.

Fig. 5. Comparative analyses of cavities between the MC2R wild type and Ala126Ser molecular models. **Panels a and b**, average structures of the 5ns time span of the trajectories for the wild type and mutant receptors, respectively. **Panels c and d**, snapshots from the molecular dynamics run retrieved at 3ns of simulation for the wild type and mutant receptors, respectively. The receptor cavities were identified using Accelrys Discovery Studio Binding Site Tools (Accelrys Inc., San Diego, CA) with a grid resolution 0.5 Å. The corresponding volumetric values for the defined regions are presented in Table 1.

Table 1. Volumes in cubic Angstrom ($Å^3$) of the major cavities identified in the MC2R wild type and Ala126Ser representative structures. Binding site numbers correspond to those displayed in Fig. 5.

Table 1. Volumes in cubic amstrongs of the major cavities identified in the MC2R wild type and Ala126Ser MD representative structures. Binding site numbers correspond to those displayed in Fig. 5.

	WT Average (a)	A126S Average (b)	WT (3ns) (c)	A126S (3ns) (d)
Site 1	848,125	262	778,5	694,25
Site 2	275,375	51,25	370,375	230,625
Site 3	103	198,875	121,25	132,25
Site 4	-	117,5	-	-
Site 5	-	94,625	-	-

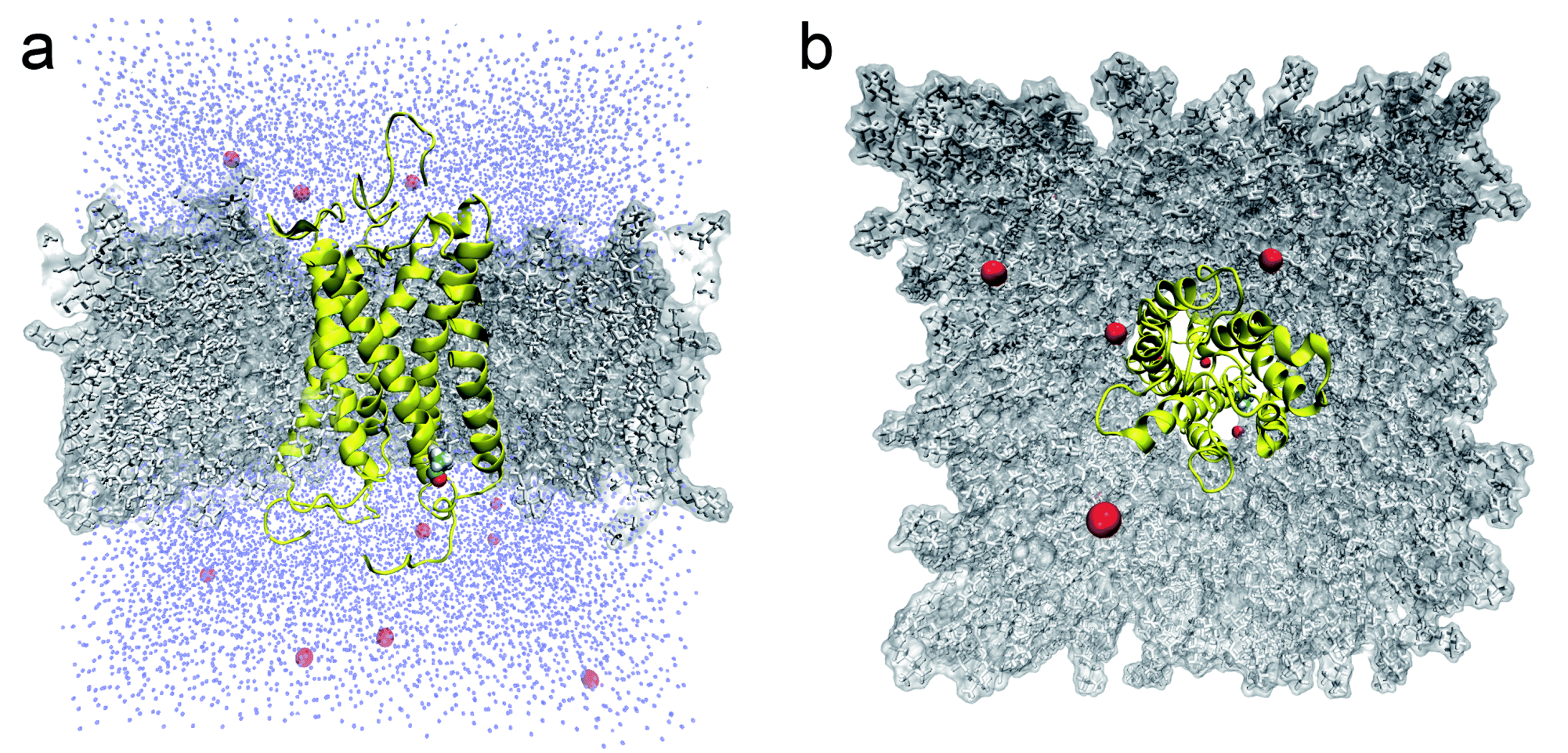
a
b

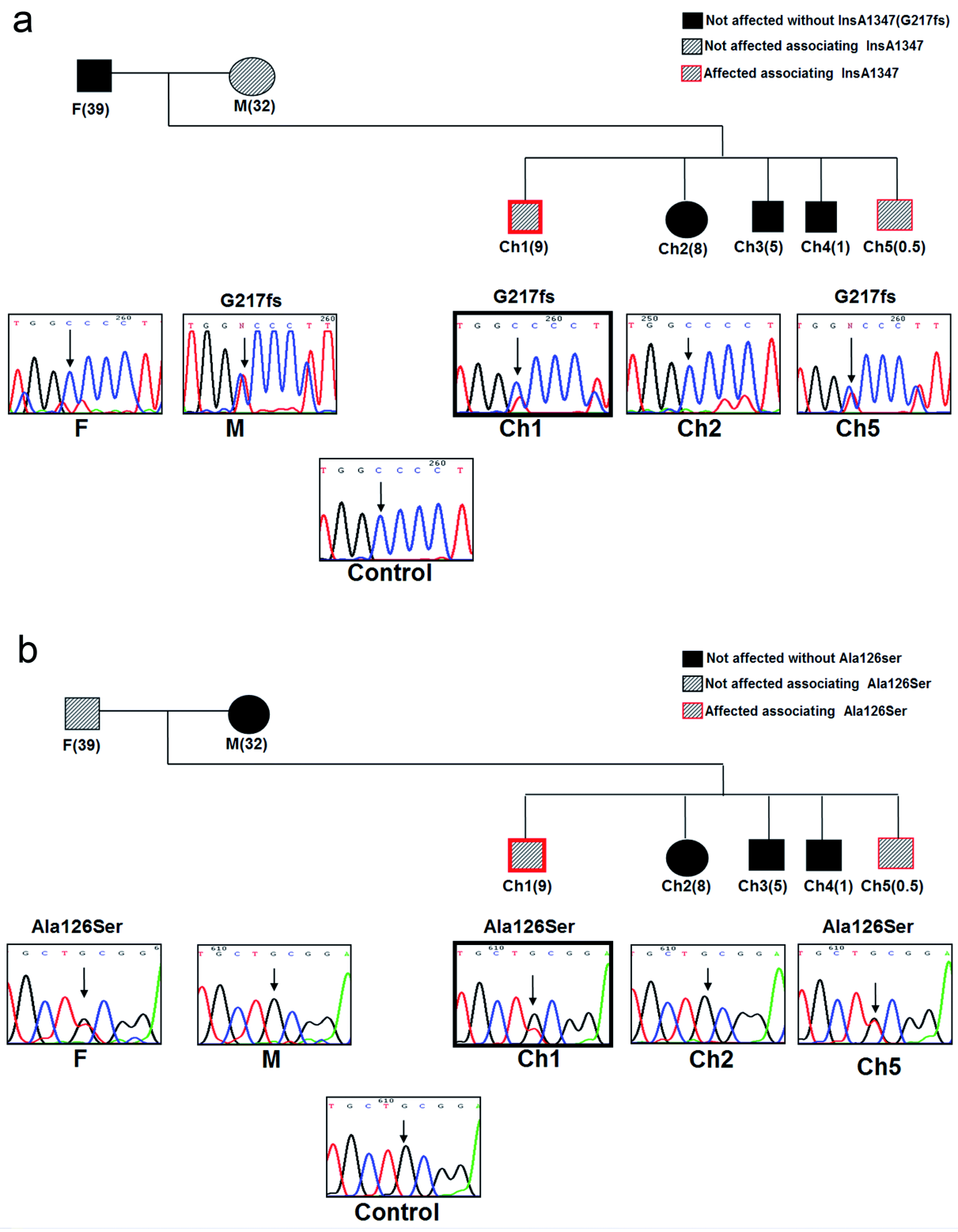
a
Not affected without InsA1347(G217fs)
Not affected associating InsA1347
Affected associating InsA1347
F(39)
M(32)
Ch1(9)
Ch2(8)
Ch3(5)
Ch4(1)
Ch5(0.5)
G217fs
G217fs
G217fs
F
M
Ch1
Ch2
Ch5
Control
b
Not affected without Ala126ser
Not affected associating Ala126Ser
Affected associating Ala126Ser
F(39)
M(32)
Ch1(9)
Ch2(8)
Ch3(5)
Ch4(1)
Ch5(0.5)
Ala126Ser
Ala126Ser
Ala126Ser
F
M
Ch1
Ch2
Ch5
Control

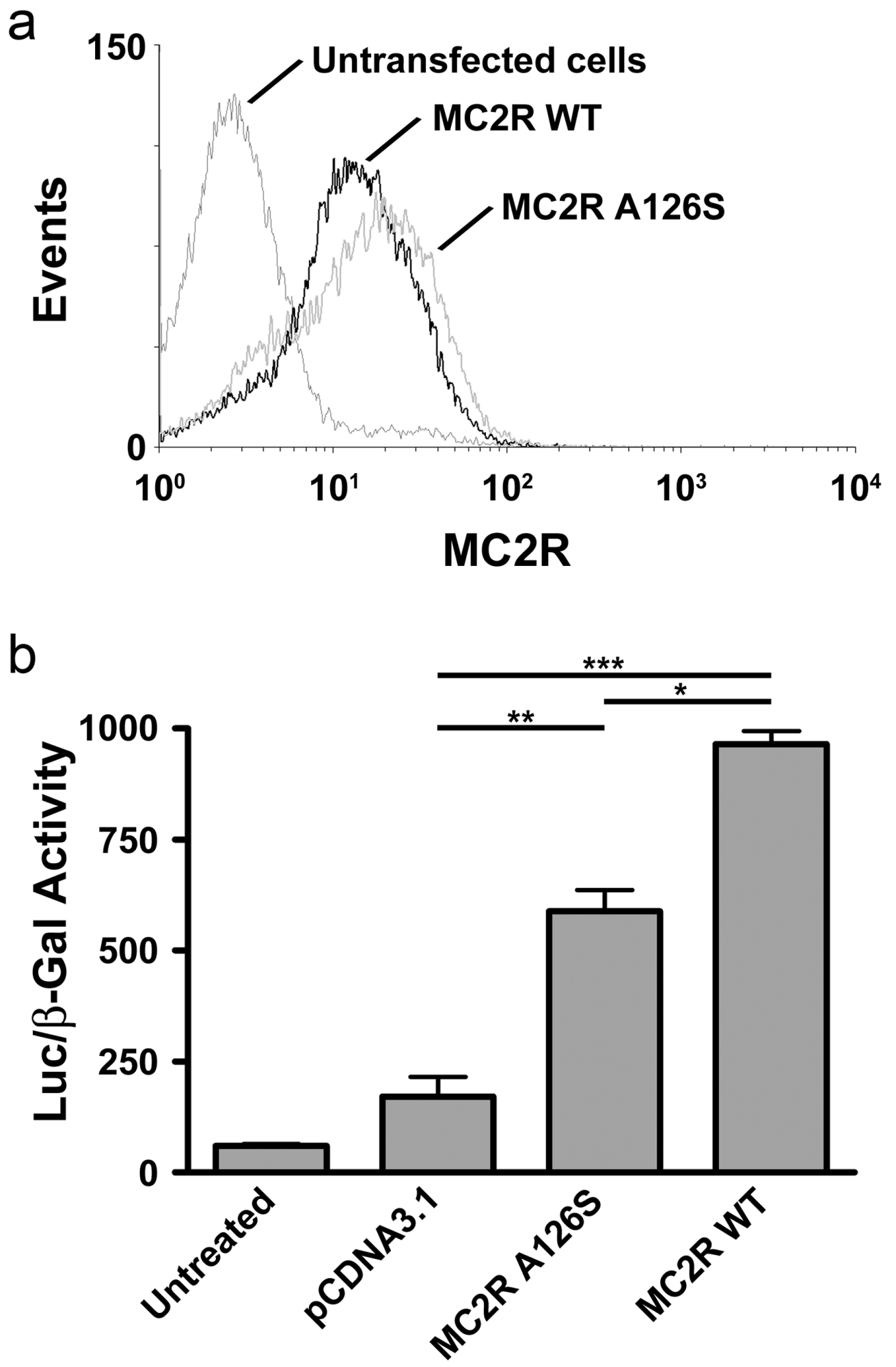
a
150
0
Events
Untransfected cells
MC2R WT
MC2R A126S
10^0
10^1
10^2
10^3
10^4
MC2R
b
***
*
**
1000
750
500
250
0
Luc/β-Gal Activity
Untreated
pCDNA3.1
MC2R A126S
MC2R WT

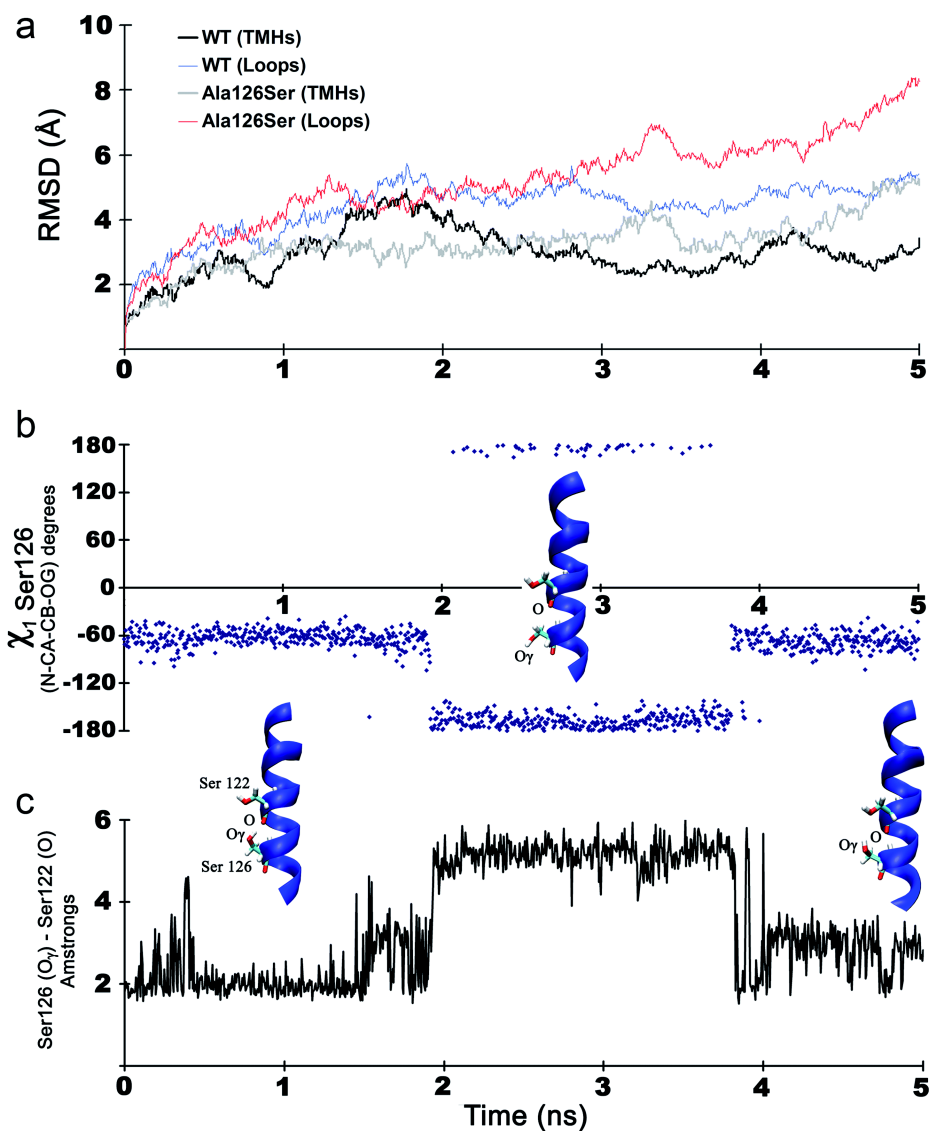
a
RMSD (Å)
WT (TMHs)
WT (Loops)
Ala126Ser (TMHs)
Ala126Ser (Loops)
b
χ1 Ser126
(N-CA-CB-OG) degrees
O
Oγ
c
Ser126 (Oγ) - Ser122 (O)
Amstrongs
Ser 122
O
Oγ
Ser 126
Time (ns)

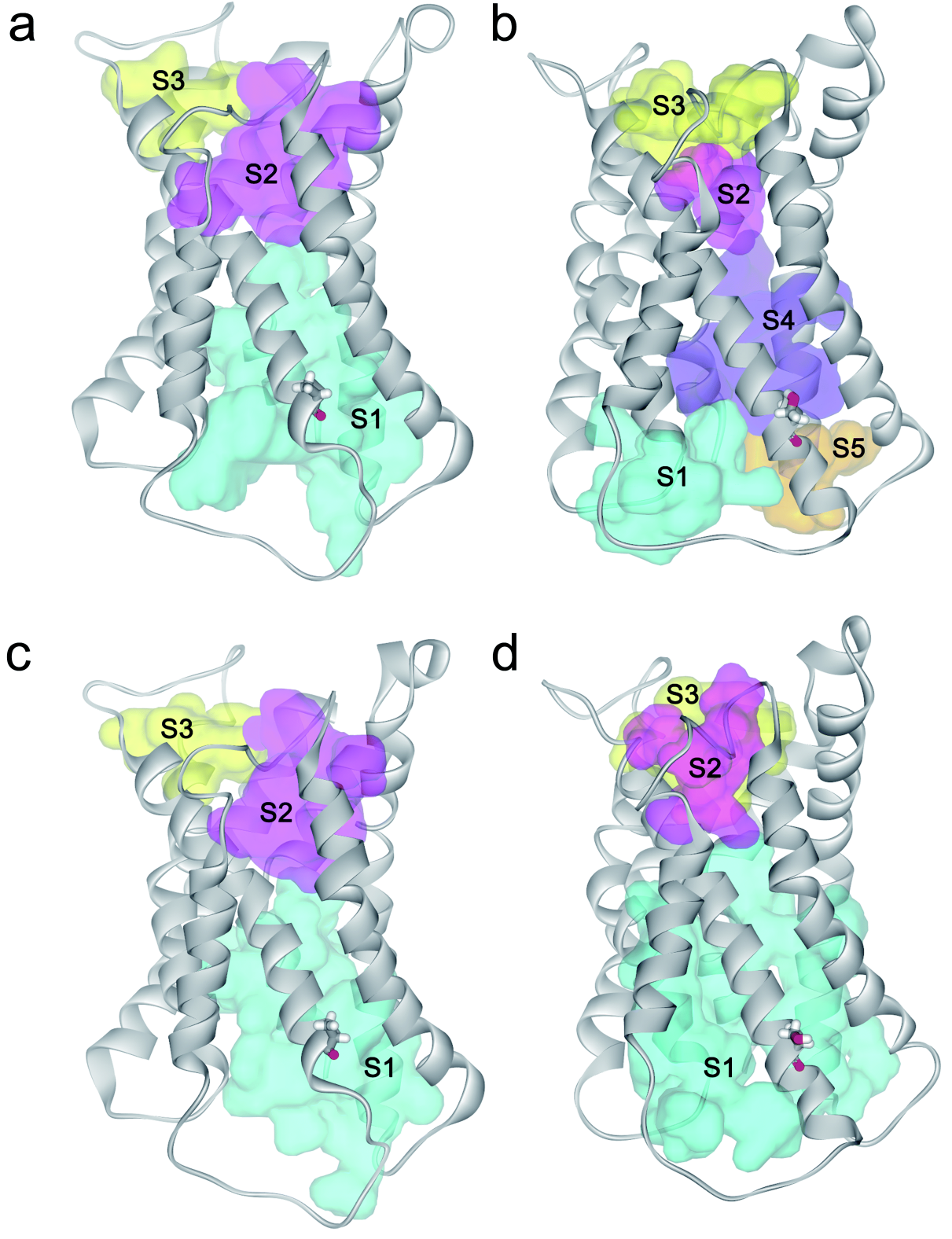
a
S3
S2
S1
b
S3
S2
S4
S5
S1
c
S3
S2
S1
d
S3
S2
S1